CGU HS Committee on River Ice Processes and the Environment
19th Workshop on the Hydraulics of Ice Covered Rivers
Whitehorse, Yukon, Canada, July 9-12, 2017.

Self-sustaining waves resulting from dynamic storage release in ice-covered channels

Spyros Beltaos
Watershed Hydrology and Ecology Research Division,
Environment and Climate Change Canada,
Canada Centre for Inland Waters,
867, Lakeshore Rd, Burlington, ON, L7S 1A1
Spyros.Beltaos@Canada.ca

The main driver of ice breakup processes is the flow discharge hydrograph. It is generated by runoff from snowmelt and rainfall but can be significantly augmented by rapid release of water from storage as the ice cover is being dislodged and broken up. There is very limited quantitative information concerning the hydrodynamic processes that control storage release during ice breakup in rivers, while the issue of climate change underscores the need for improved understanding of the relevant mechanisms. Under favourable conditions, storage release may lead to formation of self-sustaining waves (SSWs) that can rapidly mobilize and break the ice cover over long river stretches. Analysis of the results of numerical experiments in prismatic channels reveals and quantifies the main properties of the SSW, including the increase of storage-release flow and the decrease of the rate of ice clearance with increasing threshold ice-breaking discharge. It is stressed that storage release is highly transient and vanishes when ice breaking ceases. Analytical results are compared to natural stream conditions, using data from a rare occurrence of rapid ice breaking over hundreds of kilometres in Peace River (2014). This comparison indicates partial only agreement with the SSW prismatic-channel concept and shows that discrepancies may arise from the characteristic irregularity of rivers. Under certain conditions, however, the SSW concept could provide useful estimates of overall-average storage release flows. With the aid of this concept, impacts on storage release by climate- or regulation-induced changes to river ice regimes are examined along with their implications to the frequency of ice-jam formation and associated flooding.

1. Introduction

The breakup of the ice cover in cold-region rivers is a brief but important period of their hydrologic regime, with significant ecological and socio-economic implications (Burrell 2008). Major ice jams that often form during breakup can cause extreme floods that imperil human life and damage property and infrastructure (Ashton 1986). Navigation and hydro-power generation are also adversely affected by ice jamming. At the same time, ice-jam flooding can provide essential replenishment to the multitude of lakes and ponds characteristic of the northern Canadian deltas, which are havens for wildlife, especially waterfowl and aquatic animals.

The main driver of ice breakup processes is the flow discharge hydrograph. It is generated by runoff from snowmelt and rainfall but can be amplified by highly dynamic processes resulting from the rapid release of water from "storage". This results from mechanical dislodgment and subsequent breaking up of the ice cover into rubble. As shown by numerical experiments (Ferrick and Mulherin 1989; Jasek et al 2005), storage release can compensate for the natural attenuation of a wave, rendering it a self-sustaining wave, or SSW for short. It has been postulated that SSWs may play a role in rapid ice clearance that has occasionally been observed in rivers of northern Canada. An extreme occurrence took place on the Yukon River in 1983: Gerard et al (1984) reported apparent ice breaking over a 300 km stretch at an average celerity of 5.2 m/s, which reduced the intact ice cover to a 140 km long ice run.

Despite their potential importance, the properties of SSWs are not well understood, while collection of relevant field data is hampered by the fact that they travel along extensive and inaccessible river stretches. The issue of climate change underscores the need for improved understanding in this area of study because ice and flow regimes are strongly influenced by climatic variables.

The main objective of this paper is to present an analytical framework for describing the hydrodynamics of SSWs in the simple case of a prismatic channel and to consider how this knowledge may be utilized in natural streams. A secondary objective is to examine the effects of changes in ice regimes on the magnitude of flows generated by storage release.

2. Background Information

The formation of an ice cover causes river water levels to increase in order to accommodate the keel of the cover and the extra hydraulic resistance that is generated by its lower boundary. The volume of water between the prevailing and the initial (before ice cover formation) water levels is called "storage", even though the "stored" water is not stationary but moves along the river with the rest of the flow, albeit at reduced velocity. As water is being stored during the freezeup period, downstream flow is reduced and this effect is often captured in the records of various hydrometric gauges.

During the winter, the river flow typically decreases and so does the roughness of the bottom surface of the ice cover. In turn, water levels decrease and some of the stored water is released back into the flow. By the time spring runoff begins, there is a relatively small amount of water in storage, since the prevailing flow and thence the "backwater" is small. The term backwater denotes the difference between ice-covered and open-water flow depth at the same discharge.

With the arrival of mild weather in the spring (or during a mid-winter thaw), the flow begins to increase while thermal effects cause the ice bottom surface to become rougher. The backwater will increase as a result and so will the storage until the ice cover melts or is forcibly mobilized by the rising flow. In either case, there will be a release of storage, which will cause the downstream flow to increase over and above the "carrier" flow in the river. Carrier flow is the flow that is strictly attributable to runoff and prevails in the river when dynamic effects, such as javes and storage-release, are absent. In the following, the term "excess" flow will be used to denote the increment caused by storage release.

3. Ice Dislodgment and Breaking: The Self-Sustaining Wave

Highly dynamic conditions will prevail in cases where the rising carrier flow, or a sizeable jave from a released jam, dislodges and mobilizes the ice cover which then quickly breaks down into smaller slabs and blocks. At the same time, the remaining intact ice cover maintains a good portion of its mechanical strength and can, under certain geomorphic conditions, arrest the ice run and initiate ice jams ("mechanical breakup"). The release of storage counteracts the natural attenuation of the incoming wave, which has been postulated via numerical experiments to eventually become self-sustaining (Ferrick and Mulherin 1989).

Jasek et al. (2005) applied the CRISSP model to study wave propagation in ice-covered prismatic rectangular channels, assuming that ice dislodgment and breaking occur at a specified discharge (Q_{br}), which exceeded the base flow (Q_o) by varying amounts. It is known that ice dislodgment and subsequent breakup is more complex than what is envisaged by single-variable thresholds. It involves additional parameters, e.g. hydrodynamic forces applied on the ice cover, channel width and planform curvature as well as freezeup water level (Beltaos 2013). Nevertheless, the single-variable criterion greatly simplifies the study of the SSW and is rigorous for a prismatic channel, for which the critical condition could equally well be expressed in terms of velocity, depth, or shear stress.

In the CRISSP runs, dynamic conditions were generated by applying carrier flow hydrographs of different peaks and durations at the upstream boundary of the computational reach, which extended for hundreds of kilometres. If the incoming wave attained flows in excess of Q_{br}, the wave became self-sustaining after an evolutionary period; it comprised a distinct front of constant celerity, followed by a protracted crest of constant depth and discharge (herein termed peak depth and peak flow). The numerical runs indicated that the celerity of the front (C_{br}) increased as Q_{br} decreased, becoming extremely large (~10 m/s) when Q_{br} was just a little higher than the base flow. The results were also influenced by the slope of the channel bed (S_o) but not by the channel width (W).

To explore jave-induced ice breaking, which is very common in relatively flat rivers (Beltaos 2007, 2013), the writer used the model River1d (kindly provided by Prof. Faye Hicks) to study the release of a 9 km long jam in a 120 km prismatic channel of slope 0.5 m/km, width 100 m, base flow of 400 m^3/s, and bed Manning coefficient, $n_b = 0.03$. To simulate the backwater caused by the ice cover downstream of the jam, n_b was increased to 0.05 while the calculation was performed in open-water mode throughout the length of the channel. The shear stress in the "ice-

covered" reach was calculated as one-half of $\rho g Y S_f$ (S_f = friction slope; ρ = density of water = 1000 kg/m^3, g = gravitational acceleration = 9.81 m/s^2). When the shear stress at both ends of the first 1 km long "ice segment" exceeded 20 Pa, the segment was removed, i.e. n_b was reduced to 0.03 and the computation repeated using the latest water level profile as the initial condition.

Figure 1 shows that the jave quickly formed a front of constant shape and height. After 46 minutes, a short segment of practically constant depth has already developed upstream of the wave front; as time goes on, it is expected to become longer, much as was found by Jasek et al (2005). The sustained peak flow and depth were smaller than respective values associated with the initial jave (e.g. 5-minute graph). The magnitude of the celerity of the wave front (5.1 m/s) lies between those of the gravity and the kinematic waves (7.1 m/s and 1.6 m/s, respectively). The constancy of the wave front shape implies that all points along the front advanced at the same celerity and there was no attenuation. The flow depth at which the ice cover was dislodged (Y_{br}) was not much less than the sustained-peak depth (Y_p); ratio Y_{br}/Y_p = 0.89.

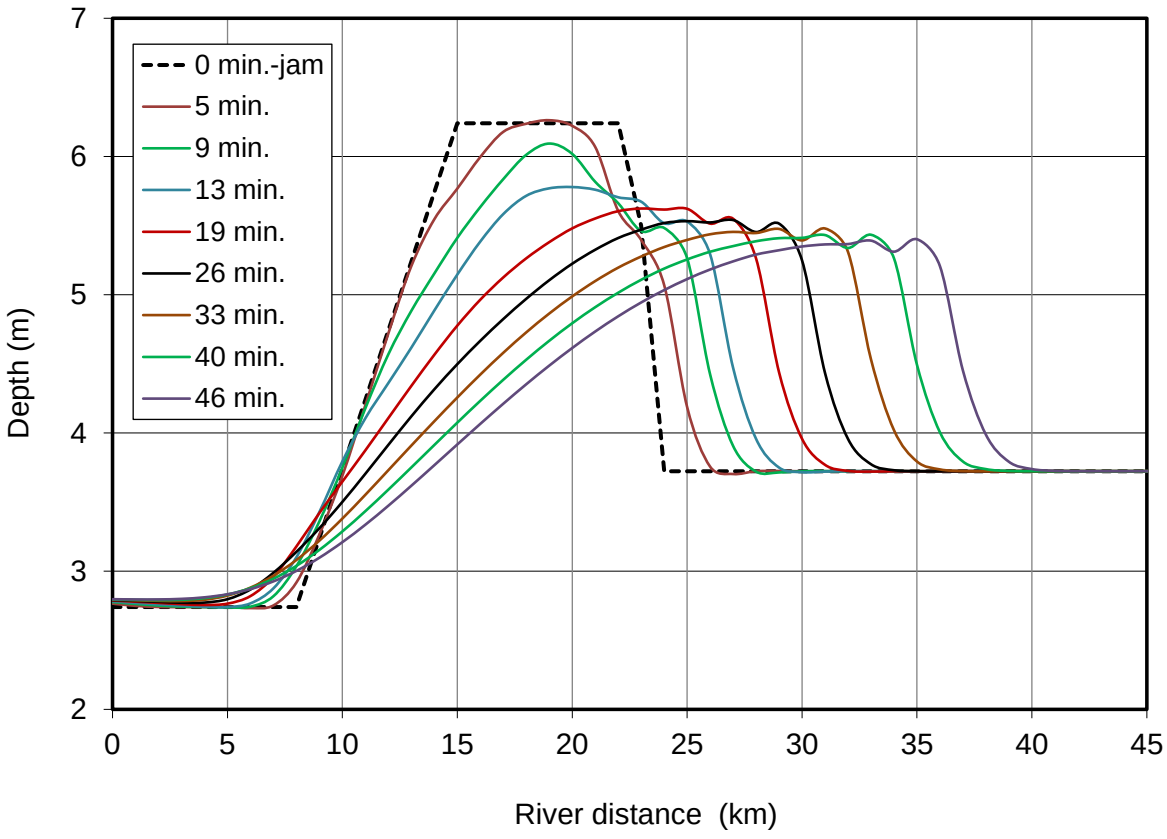

Figure 1. Longitudinal variations of water depth at different times following release of a hypothetical ice jam in a prismatic channel.

As shown by Beltaos (2017), a less dynamic type of storage release may occur as a result of frontal melt when the carrier flow is not large enough to mobilize the ice cover. In that case, the

front of the release wave continuously increases in length and propagates entirely under the intact ice cover. By contrast, the SSW wave has a sharp front of constant length and only a portion of this front is moving under intact ice.

4. Hydrodynamic Properties of Self-Sustaining Waves

With reference to the simplified sketch of Fig. 2, the one-dimensional continuity and momentum equations read (Henderson 1966):

$$\frac{\partial Y}{\partial t}+\frac{\partial q}{\partial x}=0 \qquad [1]$$

$$S_f = S_o - \frac{\partial Y}{\partial x} - \frac{1}{g}\frac{\partial U}{\partial t} - \frac{U}{g}\frac{\partial U}{\partial x} \qquad [2]$$

in which t = time; x = downstream distance; q = discharge per unit area = Q/W; S_f = friction slope, defined as total boundary resistance force per unit channel length divided by the unit weight of water and by the flow area = average boundary shear stress divided by the unit weight of water and by the hydraulic radius. Noting that C_{br} is constant along the wave front and introducing the transformation $\xi = x-C_{br}t$, Eqs 1 and 2 can be re-arranged to read

$$C_{br}Y - q = const. \qquad [3]$$

$$\frac{dY}{d\xi} = \frac{S_o - S_f}{1-\frac{(C_{br}-U)^2}{gY}} \qquad [4]$$

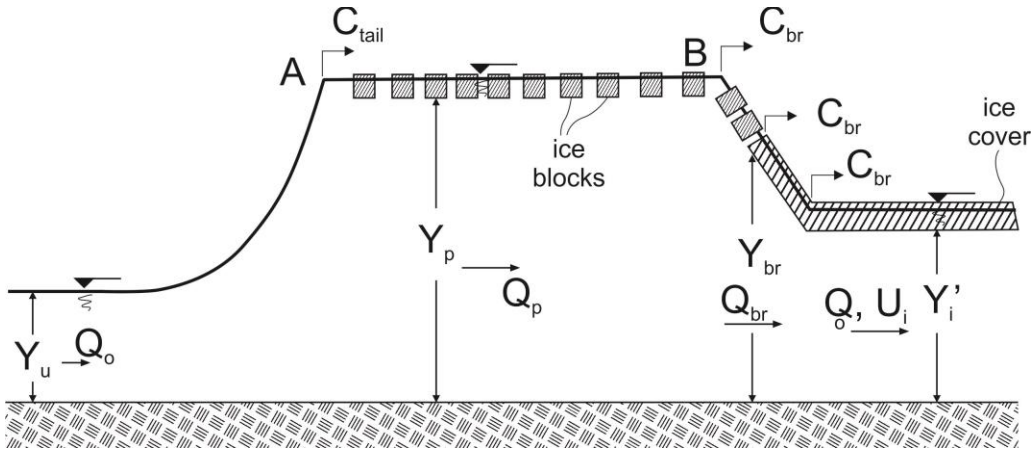

Figure 2. Schematic illustration of wave generated by sustained ice dislodgment. The wave front is depicted as a straight line segment for simplicity.

By virtue of Eq. 3, the discharge at any point along the front can be expressed as:

$$Q = Q_o + C_{br} W (Y - Y_i') \quad [5]$$

in which Y = depth of flow, measured from the bottom of the ice cover or the bottom of the moving ice floes in the open-water reach; Yi′ = depth of flow under the undisturbed ice cover downstream of the wave front. A similar relationship applies to the reach upstream of point A in Fig. 2, but here the celerity C_{tail} differs from C_{br}. Where there is no net inflow to the control volume ($Q = Q_o$ at both ends), it can be shown that

$$\frac{C_{tail}}{C_{br}} = \frac{(Y_p - Y_i')}{(Y_p - Y_u)} \quad [6]$$

Net inflow is zero in cases of jave-triggered ice breaking; for SSW initiation by a runoff hydrograph, the net inflow will become zero when the runoff discharge returns to the base value. Equation 6 indicates that $C_{tail} < C_{br}$ because $Y_i' > Y_u$. Therefore the uniform-flow crest AB will lengthen as time goes on. The few wave shapes shown in Fig. 1 only hint at this feature, which is more conspicuous in the extensive CRISSP runs (Jasek et al 2005).

Since the open-water flow in the sustained-peak reach is uniform and so is the ice covered flow beyond the wave front (Fig. 2), one can write:

$$\frac{Y_p}{Y_i'} = 2^{-2/5} \left(\frac{n_b Q_p}{n_c Q_o} \right)^{3/5} \quad [7]$$

To derive this relationship, it was assumed that the ice blocks being carried by the flow in the crest reach do not impede water motion. Jasek et al (2005) considered possible impedance by simply increasing the local value of n_b, but this resulted in implausible wave profiles.

Applying Eq. 5 to the peak flow and depth results in

$$Q_p = Q_o + C_{br} (Y_p - Y_i') W \quad [8]$$

Combining Eqs 7 and 8 results in:

$$\frac{C_{br}}{U_i} = \frac{(Q_p / Q_o) - 1}{\left[2^{-2/5} (n_b Q_p / n_c Q_o)^{3/5} - 1 \right]} \quad [9]$$

Equation 9 is confirmed in Fig. 3, in which the various data points derive mostly from the results of the numerical experiments by Jasek et al (2005). In these experiments both n_b and n_i (coefficient for ice cover) were assumed to be equal to 0.03, taking into account the thermally-

induced roughness increase of the ice cover during the pre-breakup period. For a plausible range of U_i = 0.7 to 1 m/s, SSWs are expected to advance at speeds of no less than ~2.8 m/s or ~240 km/day, since the minimum value of C_{br}/U_i is ~4 (Fig. 3). This value will change where the ratio n_b/n_c differs from 1 and can be determined using Eq. 9.

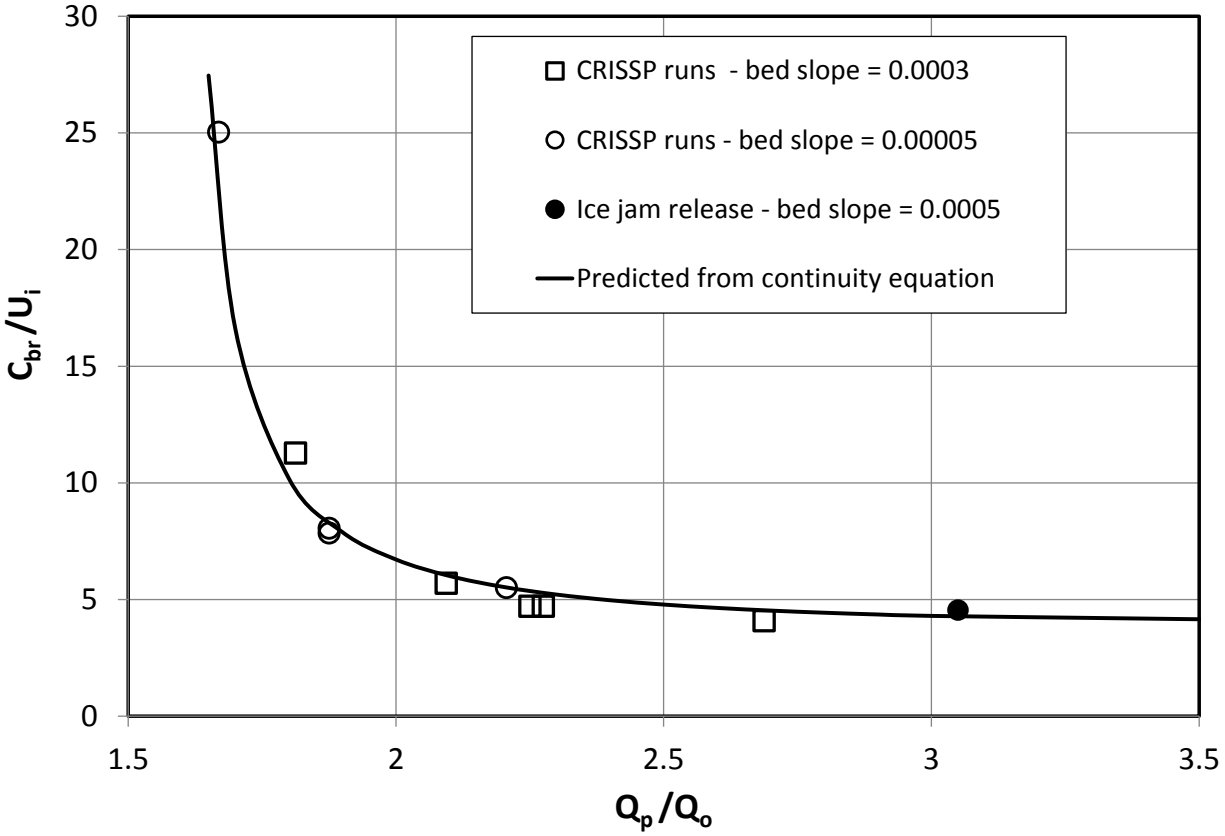

Figure 3. Normalized ice breaking celerity versus normalized peak wave discharge for n_b=n_c. CRISSP runs: Q_o = 1600 m^3/s; W = 600 m. Jam-release run: Q_o = 400 m^3/s; W=100 m. The theoretical line attains a minimum of 4.03 at Q_p/Q_o ~ 4.5.

The denominator of Eq. 9 suggests that the ratio Q_p/Q_o must exceed a limiting value to ensure that C_{br} is finite and positive. Where n_b/n_c = 1, the limiting value is equal to $2^{2/3}$ or 1.59, i.e. the excess flow due to storage release must be at least ~60% of the base flow. An additional constraint requires that C_{br} not exceed the celerity of a gravity wave (C_g) propagating in the ice covered reach downstream of the wave front (Beltaos 2017).

Figure 3 relates two hydrodynamic variables describing the SSW but is not sufficient for a full description of this waveform because the influence of the threshold discharge, Q_{br} , has not yet been quantified. Figure 4 shows that Q_p increases with increasing Q_{br}, which, by virtue of Fig. 3, implies that C_{br} should decrease with increasing Q_{br}, in agreement with what Jasek et al (2005) reported. With given Q_{br} and Q_o, one can determine Q_p from Fig. 4 and proceed to find C_{br} using

Fig. 3. The data presented in Fig. 4 indicate that excess flow can amount to 200% of the base flow and possibly more, depending on channel slope and threshold discharge.

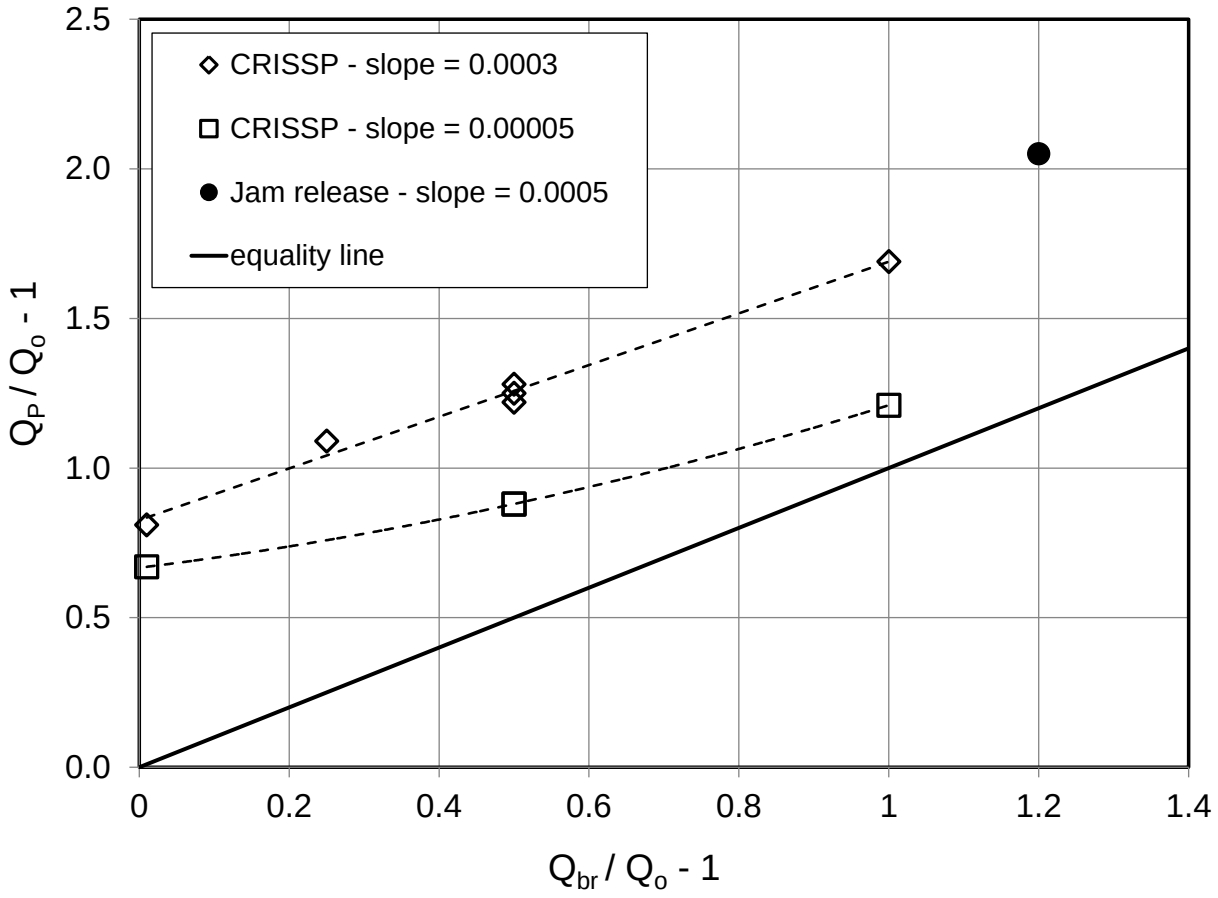

Figure 4. Dimensionless plot of excess flow caused by storage release versus threshold ice-breaking flow. Excel-generated "trendlines" for each data set are shown as dashed lines.

As noted earlier, the jave-breaking simulation indicated that the ice cover was dislodged when the under-ice flow depth, Y_{br}, was not much less than the sustained peak depth Y_p (ratio = 0.89). Jasek et al (2005) did not provide values of Y_p and Y_{br} in the tabulation of their results. However, Y_p can be calculated assuming open-water flow, as indicated previously, while Y_{br} can be determined from the equation of continuity:

$$Y_{br} = Y_i' + (Q_{br} - Q_o) / C_{br} W \qquad [10]$$

Calculated values of Y_{br} were always slightly less than those of Y_p while the ratio Y_{br}/Y_p was approximately independent of Q_{br}/Q_o for given bed slope (~0.97 and ~0.90 for S_o = 0.00005 and 0.0003, respectively, for the data of Fig. 5).

It is known that ice dislodgment and subsequent breakup is more complex than what is envisaged by single-variable thresholds. Additional parameters are involved, e.g. hydrodynamic forces applied on the ice cover, channel width and planform curvature as well as ice thickness and strength, and freezeup water level (Beltaos 2013). Nevertheless, the single-variable criterion greatly simplifies the study of the SSW and is rigorous for a prismatic channel, for which the critical condition could equally well be expressed in terms of discharge, velocity, depth, or shear stress.

5. Natural Stream Conditions: Peace River Case Study

A rare occurrence of very rapid ice clearance took place in Peace River during the 2014 breakup: ice was broken up in the lowermost 345 km of the river in a little over a day. This was triggered by a jam release in the morning of April 30 near Vermilion Chutes (located ~70 km downstream of Fort Vermilion, Alberta. The average speed of ice clearance has been estimated as 3.2 to 3.6 m/s. (M. Jasek, pers. comm. July 2016). Average hydraulic conditions for this reach are not known; data at the Peace Point Water Survey of Canada (WSC) hydrometric station (Beltaos 2011), located ~110 km above the mouth of Peace, indicate a base velocity of 0.75 m/s under the intact ice cover, while the pre-breakup value of n_i is equal to n_b (0.024); consequently, C_{br}/U_i ~ 4.3 to 4.8. This range is higher than the minimum value indicated in Fig. 3. Therefore it is possible that ice clearance was caused by a SSW.

This possibility is not, however, fully supported by the gauge record at Peace Point (Fig. 5) which indicates that not one but two waves passed by this site on May 1. Hourly time-lapse photos obtained by WSC (Fig. 6) indicate that the sheet ice cover may have shifted slightly during the night of Apr 30 to May 1. It remained stationary until at least 0701 h (MST) of May 1, even though it appeared to have shifted by tens of metres since 0601 h; at 0801 h rubble appears in the image and the ice sheet was likely in motion because its surface looks different from that of the previous photo (Fig. 7). The photos also suggest that the water level did not change appreciably between 0501 and 0701 h while there was a visible rise between 0701 and 0801 h. Wave 1 likely caused the primary orifice to re-submerge but did not break the ice cover, which remained in place until the arrival of wave 2.

The decrease of the water level following the peak suggests that wave 2 was an ordinary jave, since a SSW would have a prolonged crest, estimated to last for ~9 h (Beltaos 2017). The height and sharpness of wave 2 suggest that it was produced by release of an ice jam located not far upstream of Peace Point. The formation of this jam would have “clipped” the height and duration of wave 1 owing to water going into storage to build the backwater caused by the jam.

It is concluded that the SSW theory, as developed for prismatic channels, does not rigorously apply to rivers. Since the resistance to ice breaking varies along the river (Beltaos 2007), the threshold flow and thence the rate of ice breaking will, in reality, change over distance and time. The ice breaking front will speed up or slow down depending on local resistance characteristics. Jamming will occur where the resistance to ice breaking is high and subsequent developments will depend on how soon such jams release. Brief jamming could still fit into the theoretical SSW framework, so long as the average celerity of ice mobilization is not less than the minimum

value indicated in Fig. 3. In such instances the SSW theory could provide useful estimates of overall-average storage release flows.

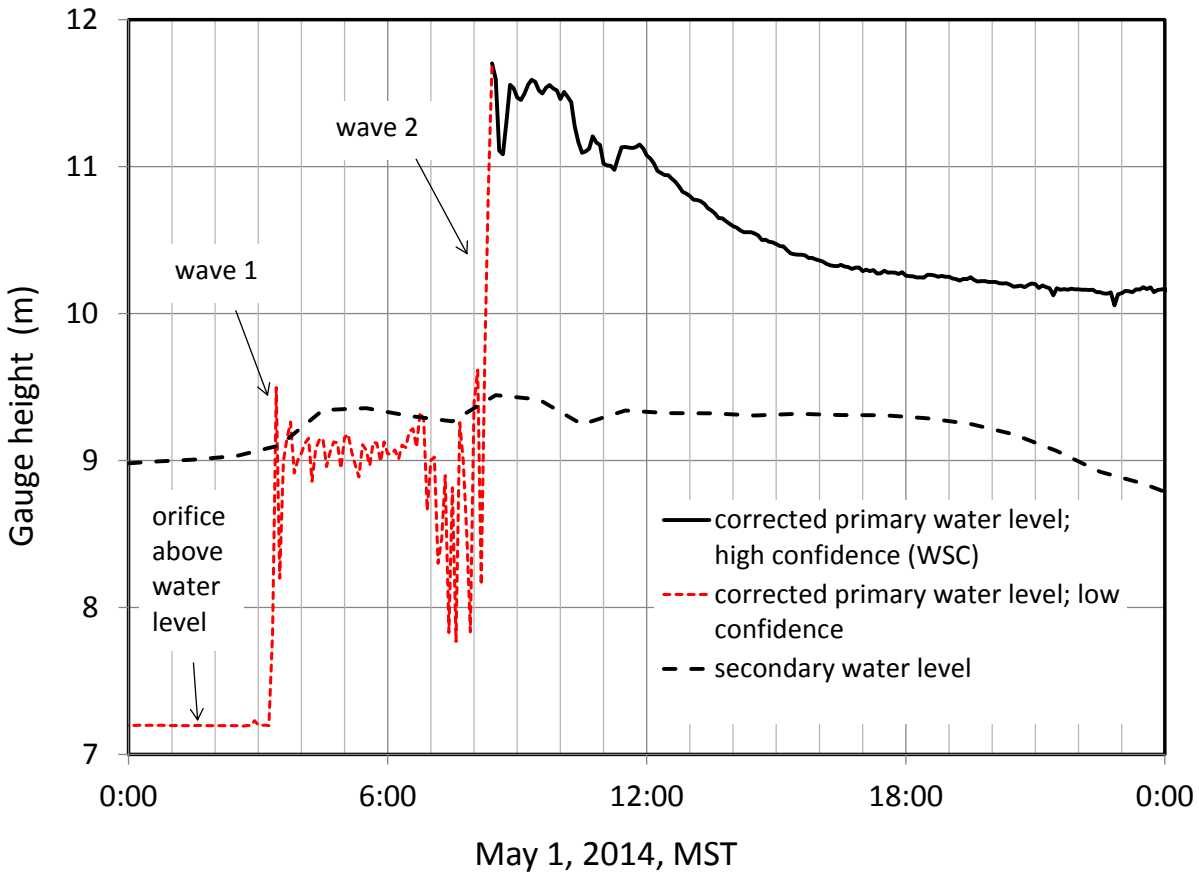

Figure 5. Hydrometric gauge record at Peace Point on May 1, 2014. Ice moved the primary orifice line on April 29 but the record was partially corrected by WSC ("high-confidence" line) by applying a constant offset after 0825 h of May 1; the "low-confidence" line, calculated by the writer using the same offset, is of unknown veracity but helpful as to the pattern of the water level variation. The secondary water level line unreliable after about 0300 h of May 1.

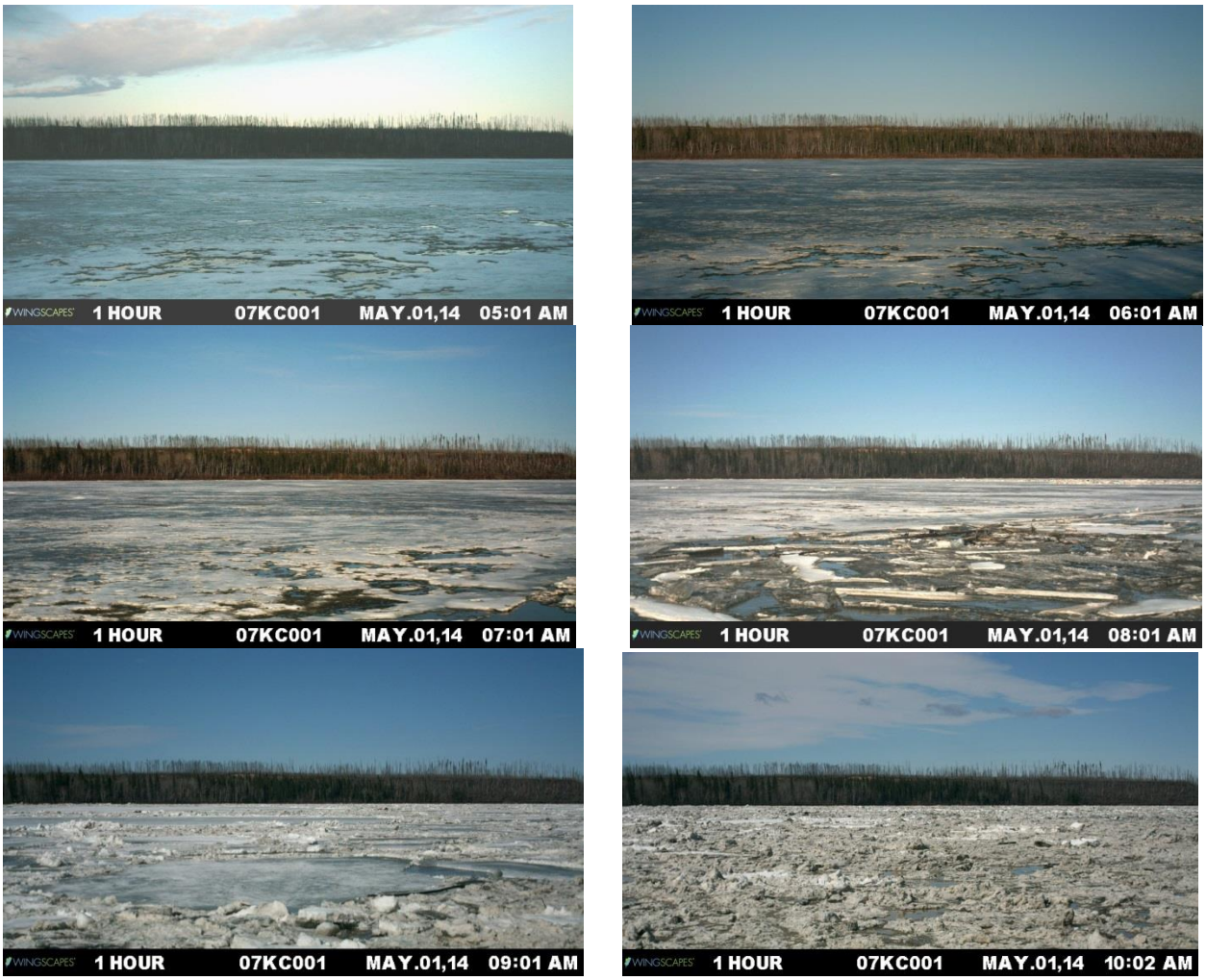

Figure 6. Peace River ice conditions at the Peace Point gauge site, morning of May 1, 2014. Flow is from right to left. Photos courtesy of Water Survey of Canada.

It is important to note that flow enhancement from storage release is a highly transient phenomenon that ends when the recession of the edge of the ice cover is discontinued. Storage release may facilitate ice breaking under certain conditions, but will cease when a sufficiently resistant ice cover is encountered by the rising flow and a jam begins to form. Downstream of the jamming point (toe of jam), the wave will continue to advance but keep attenuating unless ice breaking resumes. Upstream of the toe, water levels will rise rapidly, creating new storage and thence reducing downstream flows, as indicated, for instance, by the Peace River case study. When all of the moving ice comes to a stop, upstream and downstream flows will return to the value of the carrier river flow, which is therefore the flow that governs the potential of a jam to cause sustained flooding.

6. Effects of Changing Threshold Conditions on Storage Release

It has been shown in the preceding sections that the ice-breaking threshold parameters have a controlling influence on storage release. Therefore, it is of interest to consider how changes to river ice regimes may affect storage release flows. In this section such impacts are examined for an increase of the threshold condition, assuming that other factors are equal. This could result, for instance, from an increase in freezeup levels due to wetter fall seasons or from regulation for hydropower generation (Prowse and Conly 1998; Beltaos et al 2006; Beltaos 2014). The following reasoning applies to the likely situation in which the range of peaks of the carrier flow spring runoff hydrograph contains both present and future threshold values; it can easily be modified if this is not the case.

Let Q_{br}^P and Q_{br}^F be the present and future values of Q_{br}, such that $Q_{br}^P < Q_{br}^F$. If the highest carrier flow of the spring runoff hydrograph (Q_o^{max}), which changes from year to year, is lower than both Q_{br}^P and Q_{br}^F, it will not be possible to initiate mechanical ice breaking in either case. Instead, the breakup event will be thermal, i.e. the ice cover will largely melt in place. Ice melt will result in storage release at a rate governed largely by incoming water temperature, carrier flow, and ice thickness. Consequently, there will be no difference between present and future magnitudes of storage-release flows, which are considerably smaller than those generated by ice breaking (Beltaos 2017).

A second possibility is that of a mechanical breakup event occurring under both present and future conditions ($Q_o^{max} > Q_{br}^F > Q_{br}^P$). Fig. 4 suggests that the flow enhancement due to storage release will be greater under future than under current conditions. The difference in peak flows ($Q_p^F - Q_p^P$) will be equal to the slope of the applicable line times ($Q_{br}^F - Q_{br}^P$). In the case of the flatter channel in Fig. 4, of which the slope and width approximate the lower Peace River (Jacek and Pryse-Phillips 2015), the slope of the line is ~0.4 for the lower Q_{br} values [(Q_{br}/Q_o-1) up to ~ 0.5]. According to the analytical solution described in Beltaos (2017), this slope increases as Q_{br} increases, attaining a value of 1 for $(Q_{br}/Q_o-1) > 1.2$. If $Q_{br}^F - Q_{br}^P = 1000$ m^3/s, for instance, the flow enhancement under future conditions will be ~400 to 1000 m^3/s higher than it is under present conditions. This calculation supplies the correct magnitude of $(Q_p^F - Q_p^P)$ because it implicitly takes into account the dependency of C_{br} on Q_{br}. Appendix A shows that large errors can result when this dependency is ignored.

A mixed situation arises when the carrier flow is intermediate between present and future thresholds, i.e. $Q_{br}^F > Q_o^{max} > Q_{br}^P$. In that case, the breakup event would be thermal under future conditions and mechanical under present conditions. Storage release under future conditions would be controlled by melt and thence amount to much less than in the case of ice breaking (Beltaos 2017).

Table 1 summarizes the effects of increased threshold discharge on storage-release flow enhancement, while similar reasoning can be applied to examine the effects of reduced threshold flows. It may be further noted in Table 1 that the frequency of mechanical breakup events will be reduced by an increase in Q_{br}. Since major jams and associated floods only occur during mechanical events, their frequency would also be reduced.

Table 1. Effects of increased threshold discharge on breakup type and storage release.

Case number	Magnitude of carrier flow relative to ice-breaking thresholds	Breakup type		Effect on flow enhancement due to storage release
		Present conditions	Future conditions	
1	$Q_o^{max} < Q_{br}^{P} < Q_{br}^{F}$	thermal	thermal	no effect
2	$Q_{br}^{P} < Q_o^{max} < Q_{br}^{F}$	mechanical	thermal	negative
3	$Q_{br}^{P} < Q_{br}^{F} < Q_o^{max}$	mechanical	mechanical	positive ($\leq Q_{br}^{F} - Q_{br}^{P}$)

7. Summary and Conclusions

Storage release by ice breaking is dynamic and results in considerable additions to carrier flow, so long as it is sustained. Numerical modelling and analysis for prismatic channels suggests that ice breaking, once initiated, morphs into a SSW with constant front shape and celerity. The properties of the SSW do not appear to depend on the "trigger" flow hydrograph or jave but are largely determined by the threshold discharge, as well as base flow, ice properties, and channel hydraulics. Ice breaking celerities can be very large if the threshold discharge is close to the base flow but decrease to a minimum value of ~ 4 times the base velocity as the threshold-to-base flow ratio increases. The SSW prismatic-channel concept was only partially applicable to the extremely rapid Peace River ice clearance in the spring of 2014, a rare occurrence. It was stressed that flow enhancement by storage release is highly transient and its main effect is to potentially facilitate ice breaking farther downstream. Ice jamming at high ice-resistance sites that are invariably encountered in natural streams can disrupt the orderly advance of the wave. Nevertheless, it was suggested that the SSW concept can be useful in terms of the overall average advance of highly dynamic breakup events, so long as jamming is sufficiently brief to render the average ice breaking celerity no less than the minimum value indicated in Fig. 3. The impacts on storage release of climate- or regulation-induced changes in ice regimes can be assessed in terms of respective changes in threshold ice-breaking flows via simple reasoning that was illustrated in one example. Such changes can also modify the frequency of ice-jam flooding.

Acknowledgments

Support by Environment and Climate Change Canada to carry out this work is gratefully acknowledged. The writer would also like to thank: Professor Faye Hicks (ret. University of Alberta) for making available the model River1d; Angus Pippy and other staff of the WSC Yellowknife office for supplying archived, but unpublished, hydrometric data; and Martin Jasek of BC Hydro for sharing observational information regarding the 2014 Peace River breakup.

Appendix A. Potential Errors in Calculating the Difference ($Q_p^F - Q_p^P$)

For a specific breakup event of which the peak runoff flow exceeds both the present and future thresholds, the continuity equation (Eq. 3) can be applied near the wave front to present and future conditions, to obtain (superscripts P and F denote present and future conditions, respectively):

$$Q_p^{\,P} = Q_o + C_{br}^{\,P}(Y_p^{\,P} - Y_i')W \qquad [A1]$$

$$Q_p^{\,F} = Q_o + C_{br}^{\,F}(Y_p^{\,F} - Y_i')W \qquad [A2]$$

Similar equations can also be written for the tail end of the wave, using C_{tail} in place of C_{br} and Y_u in place of Y_i' (Fig. 3).

Subtracting Eq. A2 from Eq. A1:

$$Q_p^{\,F} - Q_p^{\,P} = \left[C_{br}^{\,F}(Y_p^{\,F} - Y_i') - C_{br}^{\,P}(Y_p^{\,P} - Y_i') \right] W \qquad [A3]$$

The latter relationship can be re-arranged to read:

$$Q_p^{\,F} - Q_p^{\,P} = C_{br}^{\,F}(Y_p^{\,F} - Y_p^{\,P})W - (Y_p^{\,P} - Y_i')(C_{br}^{\,P} - C_{br}^{\,F})W \qquad [A4]$$

Because C_{br} depends on Q_{br}, the second term on the RHS of Eq. A4 is non-zero. Large errors may result if one were to assume that C_{br} does not depend on Q_{br}. This assumption would lead to:

$$Q_p^{\,F} - Q_p^{\,P} = C_{br}^{\,F}(Y_p^{\,F} - Y_p^{\,P})W \qquad \text{(incorrect version)} \qquad [A5]$$

For the example discussed in Section 6 of the main text, the future threshold flow exceeds the present value by 1000 m^3/s. Since $Q_{br}^{\,F} > Q_{br}^{\,P}$, the difference $C_{br}^{\,P} - C_{br}^{\,F}$ is a positive number; therefore the correct difference in peak flow enhancement (Eq. A4) will be less than what is indicated by Eq. A5. As this example involves a prismatic channel that approximates the lower Peace River, one may set W ~ 600 m. Assuming that the mean flow velocity is about 1.2 m/s at the ice-breaking flow for both present and future conditions (velocity varies weakly with discharge; Leopold and Maddock 1953), the difference in ice-breaking flow depths (future minus present) is calculated as 1000/600 x 1.2 = 1.4 m. Applying a Y_{br}/Y_p ratio value of 0.97 (as determined from the CRISSP results for the flatter channel) and setting $C_{br}^{\,F}$ ~ 3.5 m/s, Eq. A5 gives $(Q_p^{\,F} - Q_p^{\,P})$ = $3.5 \times 600 \times (1.4/0.97)$ = 3030 m^3/s. This estimate exceeds by far the correct value of $(Q_p^{\,F} - Q_p^{\,P})$, which ranges from 400 to 1000 m^3/s, depending on the values of $Q_{br}^{\,F}/Q_o$ and $Q_{br}^{\,P}/Q_o$ (Section 6).

References

Ashton, G.D. 1986. *River and Lake Ice Engineering*. Water Resources Publications, Littleton, CO., USA.

Beltaos, S. 2007. The role of waves in ice-jam flooding of the Peace-Athabasca Delta. Hydrological Processes, 21(19), 2548-2559.

Beltaos, S. 2013. Hydrodynamic characteristics and effects of river waves caused by ice jam releases. Cold Regions Science and Technology 85: 42–55.

Beltaos, S. 2014. Comparing the impacts of regulation and climate on ice-jam flooding of the Peace-Athabasca Delta. Cold Regions Science and Technology, 108: 49-58.

Beltaos, S. 2017. Hydrodynamics of storage release during river ice breakup. Cold Regions Science and Technology, 139: 36-50.

Beltaos, S., Prowse, T.D. and Carter, T. 2006. Ice regime of the lower Peace River and ice-jam flooding of the Peace-Athabasca Delta. Hydrological Processes, 20 (19): 4009-4029.

Burrell, B.C. 2008. Chapter 1. Introduction. In: *River Ice Breakup*, Water Resources Publications, Highlands Ranch, Co., USA., pp 1-19.

Ferrick, M.G., and N. D. Mulherin, 1989. Framework for control of dynamic ice breakup by river regulation. Journal of Regulated Rivers: Research & Management, 3, pp. 79-92.

Gerard, R., Kent, T.D., Janowicz, R., and Lyons, R.O. 1984. Ice regime reconnaissance, Yukon River, Yukon. Proceedings of the 3rd International Specialty Conference on Cold Regions Engineering, 4–6 April 1984, Edmonton, Alta. Compiled and edited by D.W. Smith. Canadian Society for Civil Engineering, Montréal, Quebec, pp. 1059–1073.

Henderson, F.M. 1966. Open channel flow. The Macmillan Co., New York, Toronto.

Jasek, M. and Pryse-Phillips, A. 2015. Influence of the proposed Site C hydroelectric project on the ice regime of the Peace River. Canadian Journal of Civil Engineering, 2015, 42(9): 645-655.

Jasek, M., Ashton, G., Shen, H.T., and Chen, F. 2005. Numerical Modeling of Storage Release during Dynamic River Ice Break-up. Proceedings (CD-ROM) of 13th Workshop on the Hydraulics of Ice Covered Rivers, Hanover, NH, September 15-16, 2005, CGU-HS Committee on River Ice Processes and the Environment, Edmonton, Canada, 421-439.

Leopold, L.B. and Maddock Jr., T. 1963. The hydraulic geometry of stream channels and some physiographic implications. US Geological Survey Professional Paper 252, US Government printing office, Washington, 57 p.

Prowse, T. D. and Conly, M. 1998. Impacts of climatic variability and flow regulation on ice jam flooding of a northern Delta, Hydrological Processes, 12, 1589-1610.